PRISM geometric validation and DSM generation status

Junichi Takaku[(1)] **and Takeo Tadono**[(2)]

[(1)] Remote Sensing Technology Center of Japan,
Roppongi first building 7F, Roppongi 1-9-9, Minato-Ku, Tokyo, Japan, 106-0032, E-mail: takaku@restec.or.jp
[(2)] Earth Observation Research Center / Japan Aerospace Exploration Agency,
Sengen 2-1-1, Tsukuba, Ibaraki, Japan, 305-8505, E-mail: tadono.takeo@jaxa.jp

Abstract

PRISM carried at ALOS satellite is expected to generate worldwide topographic data in respects of its high resolution and stereoscopic observation. The software for generating Digital Surface Model was developed for the purpose of equipping the ground system which produces DSM semi-routinely in Earth Observation Research Center / Japan Aerospace Exploration Agency (EORC / JAXA). First, the geometric model stability and accuracy of PRISM sensor is presented with the experimental results of calibrations and validations. The geometric model of PRISM sensor consists of the static interior and dynamic exterior parameters. The interior parameters are the CCD unit camera parameters and are calibrated and validated by the preliminary experiments of self-calibrations with dense ground control points. The exterior parameters include the satellite orbit data measured by the onboard GPS receiver, the satellite attitude data measured by the onboard star tracker, gyro sensor units, and those alignment models. Those exterior parameters are calibrated and validated with adaptive orientation procedures. Next, the performance analysis of DSM generated with the PRISM geometric model is presented. The accuracy assessment results of generated DSM is presented from the comparison with high accuracy and high resolution reference DSM data sets derived from LiDAR and Aerial Photo matching at the various terrain futures.

Keywords: ALOS; PRISM; digital surface model

1. INTRODUCTION

One of the main missions of ALOS is the creation and updating of maps on a scale of 1:25,000 in Japan and other countries as the global mapping scheme. To achieve this mission precise high resolution Digital Surface Model (DSM) are necessary allover the world and PRISM performs the along-track triplet stereo observations by forward (FWD), nadir (NDR) and backward (BWD) independent optical line sensors of 2.5m ground resolution for those objectives. The correlation based triplet images matching algorithm have been exclusively developed since before the launch for this PRISM specific configurations [1], [2] and [3]. Moreover, ALOS equips GPSR and STT instruments to automatically determine exterior orientation parameters of PRISM geometry without ground control points (GCPs) [4]. This paper summarizes the current status of PRISM geometric calibration and validations, its triplet triangulation results and the accuracies of DSM generated with the triplet images matching algorithms.

2. GEOMETRIC VALIDATION

2.1. Interior orientation parameters

PRISM line sensors consist of multiple CCD units (6 units for NDR, 8 units for FWD and BWD respectively) and each CCD units have approx. 5,000 detectors (Fig. 1). The consecutive maximum 4 CCD units of each three sensor are used for the triplet stereo observations. The selection of CCD units depends on the mission operation's scenario. The interior orientation parameters are given as those CCD unit alignment data on the theoretical CCD alignment plane. The on-orbit relative accuracy of those alignment data between CCD units was evaluated and calibrated as the self-calibration. GCP residuals of exterior orientations including dense GCP test site [5] were statistically analyzed for the on-orbit self-calibrations. The systematic residuals along CCD units were modeled with the linear regressions and the alignment data were calibrated. The alignment errors of each boundary between the CCD units were calibrated with the sub-pixel image matching on overlapping 32 pixel data. Fig.2 shows the exterior orientation residuals of NDR image with 3,095 GCPs (118 scenes) vs. pixel address of CCD units on image space as the accuracy of the calibrated CCD alignment data. Table 1 shows the residuals sigma on image space for FWD, NDR and BWD respectively.
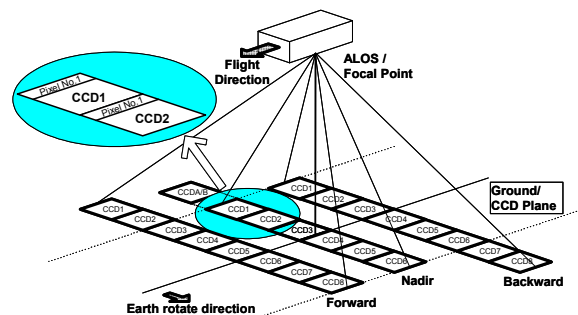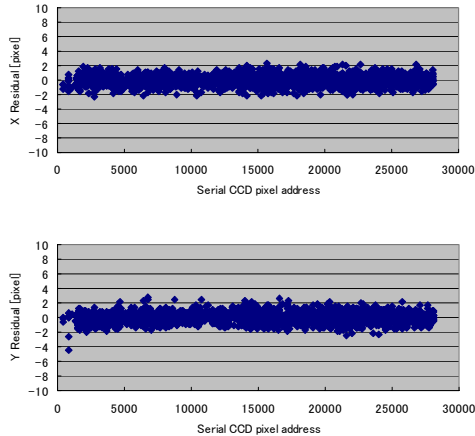

Figure 1.   PRISM CCD units configuration

Figure 2. GCP residuals of exterior orientations vs. pixel address of CCD units (NDR) on image space

Table 1. GCP residuals sigma on image space [pixel]

FWD 105 scenes		NDR 118 scenes		BWD 117 scenes	
2,648 GCPs		3,095 GCPs		2,901 GCPs	
X sigma	Y sigma	X sigma	Y sigma	X sigma	Y sigma
0.80	0.70	0.65	0.65	0.66	0.72

2.2. Exterior orientation parameters

The accuracy of positional elements determined by on-board GPSR data was confirmed within the spec accuracy (1m [4]) by validations of SLR stations. However, the pointing elements determined by on-board STT data and PRISM sensor alignment against STT have not yet satisfied the spec accuracy (2.0e-4 degree [4]). The major factor of the pointing errors is the sensor alignment changes depending on thermal conditions. We tried to model those alignment changes as the short term and long term trends. The short term parameter is the orbit cycle parameter 's' which is a normalized parameter of the ratio of time from opening of a satellite eclipse to orbit cycle period (98.7min.). The orbit cycle corresponds to major changes of satellite thermal conditions. The long term parameter is the date of observation and it corresponds to minor changes of satellite thermal conditions. Euler angles (roll, pitch and yaw) of sensor alignment errors were analyzed and it was confirmed that yaw angle is negligible. The 2nd degree Fourier series was applied to the short term trend and the linear model was applied to the long term roll trend and the 2nd degree polynomial was applied to the long term pitch trend as the results of preliminary analysis. Fig. 3 shows the short and long term trend model fitting results of roll and pitch errors estimated with exterior orientations of 97 BWD scenes. The fitting residuals sigma for FWD, NDR and BWD sensors are shown in table 2.

2.3. Triangulation accuracies

3-D (XYZ) measurement accuracies of triplet stereo triangulations were evaluated with 10 sample scenes which were observed from 03/23/2007 to 09/06/2007. 9 tie points were measured manually for each triplet stereo scene. A basic variation of number of GCP is 0, 1, 9 and 25 points

and possible large number of GCP was evaluated for each scene. Only relative orientation was performed for GCP-0 model and its accuracies depend on the sensor alignment trend model described in previous section. Roll and pitch bias of sensor alignment errors were corrected for GCP-1~25 models. The accuracies were evaluated with the independent check points which were not used as the control points. Fig. 4 shows the XY-RMSE as the planimetric accuracies and Fig. 5 shows the Z-RMSE as the height accuracies of triangulations. The planimetric accuracies are less than 8m RMSE and the height accuracies are less than 10m RMSE except for 1 scene without GCP (GCP-0). And only 1 GCP improve the XYZ accuracies to <3m with correcting only sensor alignment roll and pitch errors.
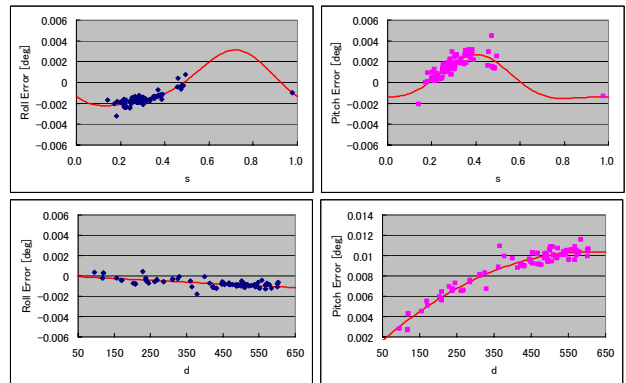

Figure 3. Trend model fitting results (BWD 97 scenes)

Table 2. Trend model fitting residuals

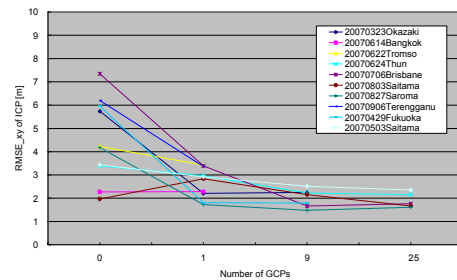|	No. of Scenes	Residuals (sigma) [deg]		@ ground level [m]	
		Roll	Pitch	CT	AT
FWD	88	0.000512	0.000453	6.18	6.84
NDR	102	0.000373	0.000410	4.50	4.95
BWD	97	0.000281	0.000522	3.39	7.88

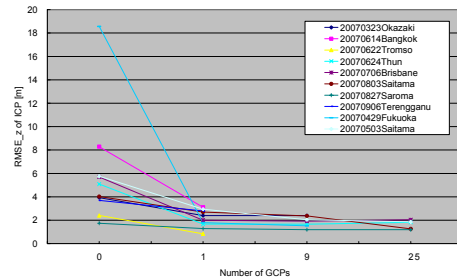
Figure 4. Triangulation accuracies (planimetry)

Figure 5. Triangulation accuracies (height)

3. DSM GENERATION

DSM generating algorithm is the correlation based triplet stereo images matching algorithm exclusively developed for PRISM [1], [2], [3]. In this paper, generated DSM accuracies of four scenes selected from the samples of triangulation accuracies evaluation which is described in section 2.3. Six reference DSM sites are included in those four scenes. The list of those stereo images is summarized in table 3 and the specs of reference DSM data sites are shown in table 4 and Fig. 6. The generated DSMs of scene 1, 2, 3 and 4 are shown in Fig. 7, 8, 9 and 10 respectively. The DSM grid is 10m (4 pixels) in image frame, then resampled to 0.3 arc-sec geodetic latitude-longitude frame. Reference DSMs were resampled to same frame (0.3 arc-sec latitude-longitude) and height differences were calculated as the height accuracies. Water (i.e. sea, large liver or lake) areas were masked as dead areas by preliminary manual editing and excluded from validations. No manual correction was made on generated DSMs. No initial DEM/DSM was used for the matching procedure. The accuracies of DSMs generated with 0-GCP and all-GCP models are compared. The DSM height accuracies of each reference DSM site are summarized in table 5. The bias errors of DSM height are almost consistent with the triplet triangulation accuracies. As the all-GCP model's results, the height accuracy is 5.1m RMSE in flat Saitama site which includes the paddies and urban terrains, and are 5.9~7.4m RMSE in Fukuoka, Thun, and Bern sites which include mixed various terrains i.e. mountains, farms, cities, etc., and are 5.8~8.2m RMSE in mountainous Okazaki and SW sites.

Table 3. Test scenes (triplet stereo)

No.	Ref. DSM Sites	Obs. Date	No. of GCPs	No. of TPs
1	Okazaki	2007/3/23	17	9
2	Fukuoka	2007/4/29	24	9
3	Saitama	2007/5/3	213	9
4	Thun /SW/ Bern	2007/6/24	54	9

Table 4. Reference DSM data sites

Site	Source	Size	Height Range	Ground Resolution	Height Accuracy	Source Year
Saitama[*1)]	LiDAR	14.0x12.0km	100m	1m	<1m	2002
Fukuoka[*1)]	LiDAR	12.0x9.0km	500m	1m	<1m	2002
Okazaki[*1)]	Aerial Photo	6.0x6.0km	400m	10m	~10m	2005
Thun[*2)]	Aerial Photo	7.5x14.5km	500m	2.5m	0.5~2.5m	2004
SW[*2)]	Aerial Photo	7.5x14.5km	1000m	2.5m	0.5~2.5m	2004
Bern[*2)]	Aerial Photo	11.0x11.5km	400m	2.5m	0.5~2.5m	2004

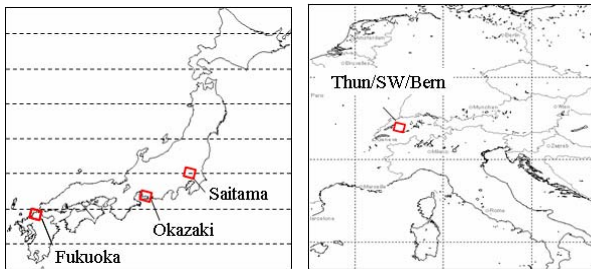*1) provided by GSI / *2) provided by ETH

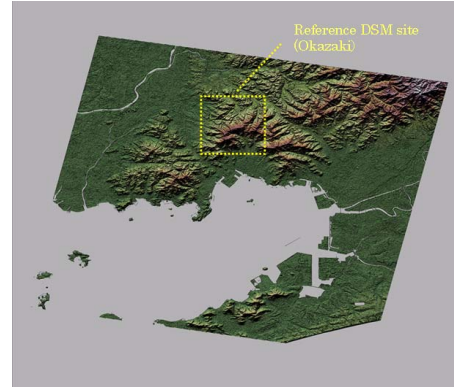*Figure 6. Reference DSM site locations*
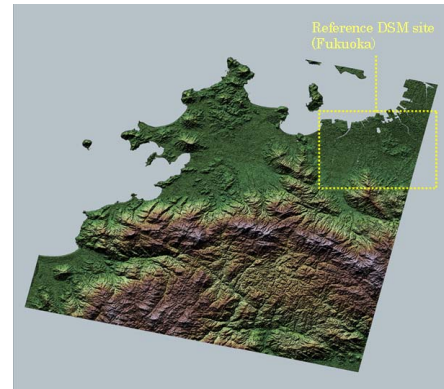

Figure 7. PRISM-DSM of scene 1

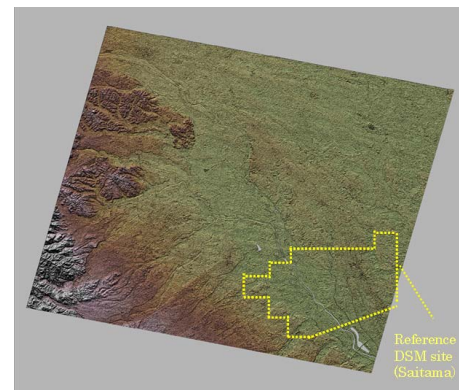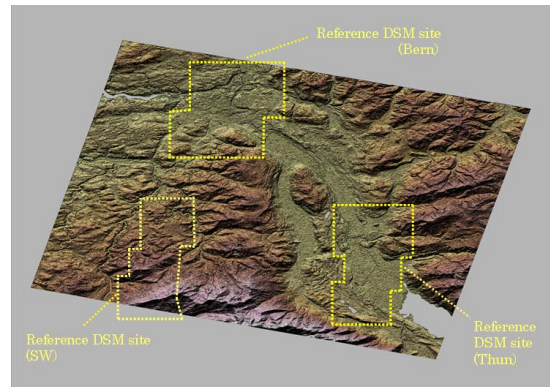*Figure 8. PRISM-DSM of scene 2*

Figure 9. PRISM-DSM of scene 3

Figure 10. PRISM-DSM of scene 4

Table 5. Height accuracies of PRISM-DSM

Site	Terrain	Model	Points	Bias [m]	SD [m]	RMSE [m]	Max [m]	Min [m]
Okazaki	Mountainous	0-GCP	548352	-3.22	5.98	6.79	101	-90
		17-GCP	548352	0.27	5.82	5.82	101	-90
Fukuoka	Various	0-GCP	1177679	-16.44	7.13	17.92	93	-226
		24-GCP	1178376	2.20	7.05	7.39	117	-210
Saitama	Frat & Urban	0-GCP	1505333	6.93	4.91	8.50	83	-173
		213-GCP	1505512	1.47	4.88	5.09	83	-178
Thun	Various	0-GCP	1672561	-6.13	5.80	8.44	98	-121
		54-GCP	1672585	-1.29	5.78	5.92	98	-114
SW	Steep Mountain	0-GCP	1163012	-5.57	8.19	9.91	86	-138
		54-GCP	1163166	-0.83	8.13	8.17	114	-128
Bern	Various	0-GCP	2015821	-6.73	6.93	9.66	71	-77
		54-GCP	2015505	-1.89	6.95	7.20	78	-88

Table 6. DSM height accuracy depending on terrain characteristics

Site	Terrain	Points	Bias [m]	SD [m]	RMSE [m]	Max [m]	Min [m]
Saitama	Paddy1	17892	0.48	2.73	2.77	22	-16
Saitama	Paddy2	3287	-0.57	1.75	1.85	9	-12
Saitama	Urban1	24424	3.18	9.78	10.28	64	-120
Saitama	Urban2	16029	1.06	17.10	17.13	76	-171
Saitama	City1	25665	1.14	4.08	4.23	40	-22
Saitama	City2	19695	1.12	3.97	4.12	37	-38
Okazaki	Dense Trees1	31243	-0.92	6.32	6.38	48	-72
Okazaki	City1	7155	1.25	2.51	2.80	18	-29
Okazaki	City2	5680	0.98	3.56	3.69	32	-25
Okazaki	Paddy	8023	0.68	2.45	2.55	18	-14
Okazaki	Dense Trees2	14940	-0.46	4.77	4.79	29	-31
Thun	Sparse Trees	5112	3.18	7.58	8.22	35	-25
Thun	Grass Field	6120	-0.77	6.80	6.85	31	-35
Bern	Dense Trees	7800	-3.81	6.13	7.22	19	-40
Bern	City	19431	-1.67	4.72	5.01	38	-32
SW	City	7599	-1.78	2.96	3.45	18	-27
SW	Truck Farm	7560	-3.59	6.87	7.75	38	-55
SW	Dense Trees	6930	9.65	14.80	17.67	90	-19

The height accuracy dependence on terrain characteristics was evaluated with manually selected local areas in all-GCP model DSMs. The selected areas and their height accuracies are summarized in table 6. The best accuracies were acquired at flat open paddy areas. However, the accuracies fall down even in flat areas depending on the terrain textures (i.e. grass, farm). It seems that the noises of JPEG compression (1/4.5) applied to PRISM data downlink format affect to the accuracies. The worst accuracies were acquired in urban and tree areas. In urban areas, high (>approx.20m) building heights could not be extracted depending on the floor size of them and the modeling errors like smoothed building edges cause the height errors (Fig. 11). Almost errors of site Fukuoka and Saitama were caused by those high building areas. In some tree areas, the canopies heights seem not to be extracted accurately (Fig. 12). One possible explanation of those errors is a seasonal change between reference DSM and PRISM images. Also the density of trees seems to be correlated to whether the canopies or the ground heights are extracted. Almost errors of site Okazaki, Thun, SW and Bern were caused by those tree area's height differences.

4. CONCLUSION

The current status of PRISM geometric validations and DSM generations were presented. The geometric interior parameters were validated by on-orbit self-calibrations and the trends of geometric exterior parameters along thermal conditions were analyzed for GCP free orientations. The triangulation accuracies without GCP were 8m and 10m for planimetry and height respectively and they can be improved to ~3m with only 1 GCP. The height error biases of generated DSMs were consistent with those triangulation results. We believe that those height offsets without GCP can be reduced by further investigations of geometric exterior parameter's error trends. The RMSE of generated DSMs were 5m for flat areas and 6~7m for mixed various terrain areas and 6~8m for mountainous areas. Large errors of DSMs were focused on high building urban areas and dense tree areas. Those height accuracies may be improved if the image quality (i.e. JPEG noise) is refined.
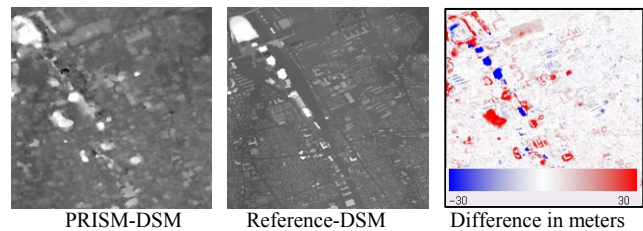
Acknowledgement

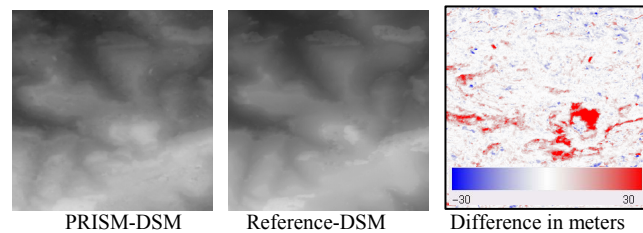Figure 11. Urban2 (approx. 2x2km) in Saitama

Figure 12. Dense trees (approx. 2x2km) in SW

References

[1] J. Takaku et al, "High resolution DEM generation from ALOS PRISM data - triplet image algorithm evaluation -," Proceedings of IGARSS03 Toulouse, France, 2003.

[2] J. Takaku et al, "High resolution DEM generation from ALOS PRISM data - Simulation and Evaluation -," Proceedings of IGARSS04 Anchorage, USA, 2004.

[3] J. Takaku et al, "High resolution DSM generation from ALOS PRISM data - Pre-launch Simulation and Assessment Plans -," Proceedings of IGARSS05 Seoul, Korea, 2005.

[4] T. Iwata, "Precision Geolocation Determination and Pointing Management for the Advanced Land Observing Satellite (ALOS)," Proceedings of IGARSS03 Toulouse, France, 2003.

[5] T. Tadono et al, "Calibration and Validation Plans of ALOS Optical Sensors," Proceedings of IGARSS04 Anchorage, USA, 2004.